Slow molecular dynamics of water in a lyotropic complex fluid studied by deuterium conventional and spin-lattice relaxometry NMR

C. R. Rodríguez and D. J. Pusiol
Facultad de Matemática, Astronomía y Física, Universidad Nacional de Córdoba, Ciudad Universitaria, X5016LAE, Córdoba, Argentina

A. M. Figueiredo Neto
Instituto de Física, Universidade de São Paulo, Caixa Postal 66318, 05315-970 São Paulo, Brazil

R.-O. Seitter
Sektion Kernresonanzspektroskopie, Universität Ulm, 89069 Ulm, Germany
(Received 28 August 2001; published 8 February 2002)

A nuclear magnetic resonance study of protons and deuterons in the mesomorphic phases of the micellar lyotropic mixture potassium laurate/1-decanol/heavy water is reported. The slow dynamical behavior of water molecules has been investigated with deuterons spin-lattice relaxation dispersion in the Larmor frequency range $10^3 < \nu_L < 4.2\times10^7$ Hz. In order to compare relative behaviors additional T_1 dispersion of micellar protons has been measured in the same compound, temperature, and Larmor frequency range. From the experimental behaviors, we conclude that in the nematic phases the water slow reorientational dynamics is closely related to the slow reorientation of the micellar aggregates. In addition, conventional deuterium nuclear magnetic resonance at $\nu_L = 4.2\times10^7$ Hz spectra has been measured at different places in the phase diagram. The line shapes show a quadrupolar splitting in nematic phases, meanwhile in the isotropic phase the spectral structure collapses in a single line. This indicates that in the nematic phases the water reorientations are not enough to average the deuterons quadrupolar Hamiltonian. On the other hand, fast isotropic water reorientations reduce the quadrupolar interactions in the isotropic phase.

DOI: 10.1103/PhysRevE.65.031703 PACS number(s): 61.30.Eb, 61.30.Gd, 76.60.Gv, 76.60.Es

I. INTRODUCTION

Amphiphilic molecules present two well-defined regions in their structure that are known to be, respectively, polar and nonpolar. Once this kind of molecules are mixed with a solvent, above the critical micellar concentration, hydrophobic-hydrophilic interactions drive the molecules to form a macroscopic anisotropic complex fluid known as *lyotropic liquid crystal* (LLC) [1]. Studies of lyotropics are of great interest since they have well-defined physical-chemical properties in all their different phases and can be used as models for biological systems. It is known that the state of water—the solvent—in such systems is different from that of ordinary bulk water and that it plays a dominant role in biochemical reactions and cellular events [2].

On the microscale, the structures of the various LLC phases are similar and three regions of the system are clearly identified [3]: (i) *Region 1* consists essentially of hydrocarbon chains, where only small amounts of water and counterions may be dispersed; (ii) *Region 2* is an interface region where the relatively immobile polar head groups are located, they interact strongly with the solvent and the counterions; (iii) *Region 3* is formed by intermicellar water, some counterions and a small amount of amphiphilic monomers.

The understanding of water dynamics in a broad time scale is essential for relating the dynamical properties of water to micelles (or membranes) dynamics. In a previous work, we studied the slow dynamics of micelles in the lyotropic micellar mixture potassium laurate (KL)/1-decanol (DeOH)/water (D_2O) [4]. Here, we report a study of the slow dynamics of water in the same ternary mixture by using deuterium NMR (nuclear magnetic resonance) longitudinal relaxometry, covering a range of several orders of magnitude in the Larmor frequency. The work is completed with the study of the deuterium electric quadrupolar interaction as it is reflected on the NMR line shape in all the mesomorphic structures present in the lyotropic phase diagram [5,6]. The water dynamics is discussed in terms of the two-step processes model proposed by Halle and Wennerström in Ref. [7].

II. EXPERIMENTAL SECTION AND METHODS

A. Sample preparation and characterization

Potassium laurate was synthesized in the laboratory from lauric acid and potassium hydroxide and recrystallized (three times) from absolute ethanol. All the basic compounds were Merck supplied. The molecules forming micelles were mixed at the fixed ratio [KL]/[DeOH] = 4 (where [ ] states for the weight percentage (wt %) of the compound) and deuterated water (Merck purity 99.8%) was added in adequate proportions to prepare samples at 66, 67, and 68 wt % of D_2O. The compounds were mixed for 2 h in a commercial ultrasound bath. The finally prepared samples were labeled according to their respective water concentrations as TD1, TD2, and TD3, respectively.

The phase diagram of this ternary mixture shows three different nematic phases [5], two of them are uniaxial (calamitic N_C and discotic N_D), depending on whether the di-

TABLE I. Transition temperatures corresponding to the investigated samples.

Sample	Phases and transition temperatures
TD1	$\mathrm{POL} \overset{\sim 22.5\,^\circ\mathrm{C}}{\rightarrow} \mathrm{N}_B \overset{\sim 32\,^\circ\mathrm{C}}{\rightarrow} \mathrm{ISO}_1$
TD2	$\mathrm{ISO}_2 \overset{\sim 9.5\,^\circ\mathrm{C}}{\rightarrow} \mathrm{N}_D \overset{\sim 16\,^\circ\mathrm{C}}{\rightarrow} N_B \overset{\sim 22\,^\circ\mathrm{C}}{\rightarrow} \mathrm{N}_C \overset{\sim 39\,^\circ\mathrm{C}}{\rightarrow} \mathrm{ISO}_1$
TD3	$\mathrm{ISO}_2 \overset{\sim 9.0\,^\circ\mathrm{C}}{\rightarrow} \mathrm{N}_D \overset{\sim 19\,^\circ\mathrm{C}}{\rightarrow} \mathrm{N}_B \overset{\sim 21\,^\circ\mathrm{C}}{\rightarrow} \mathrm{N}_C \overset{\sim 41\,^\circ\mathrm{C}}{\rightarrow} \mathrm{ISO}_1$

rector $\mathbf{n}(\mathbf{r})$ orients, respectively, parallel or perpendicular to the external NMR Zeeman magnetic field ($\mathbf{B}$), and the third one is biaxial (N_B). Those phases are surrounded by a high temperature isotropic (ISO_1) phase and another reentrant low temperature isotropic (ISO_2) one. The transition temperatures corresponding to the prepared samples are shown in Table I. They were measured and the phases identified by using differential thermal scanning, texture observations, and x-ray-diffraction techniques.

The micelles are supposed to be intrinsically biaxial platelets [6], having approximately the same shape in the three nematic and neighboring isotropic phases with, three orthogonal symmetry axis [1] of order 2. The dimensions of the micelles in the middle of the N_B region, were estimated as [1] 8.5, 5.5, and 2.6 nm, where the smallest value corresponds to the amphiphilic bilayer. The dimensions reserved for the intermicellar water are about 2.5 nm in the three orthogonal directions. This corresponds to about five or six water layers between micelles.

B. ^{2}H-spectra and ^{1}H and ^{2}H$-T_1(\nu_L)$ measurements

The line shape experiments were performed in a standard Bruker MSL 300 spectrometer in the temperature range ($11\,^\circ\mathrm{C} \leqslant T \leqslant 45\,^\circ\mathrm{C}$), within an accuracy better than 0.5 K. The measurements of the longitudinal ^{2}H relaxation time T_1 as a function of the Larmor frequency ($10^2 \leqslant \nu_L = \omega_L/2\pi \leqslant 10^6$ Hz) and temperature range ($20\,^\circ\mathrm{C} \leqslant T \leqslant 45\,^\circ\mathrm{C}$) were carried out at a Larmor frequency variable fast field-cycling NMR relaxometer. Details about the underlying techniques, in particular, the performance of field-cycling measurements of the T_1 relaxation dispersion, have been previously described in Ref. [8]. In order to assure the stabilization of the sample temperature in each phase, we waited for about one hour after each temperature variation had been performed.

III. THEORY

A. Relaxation models of micellar systems

We summarize here some relevant aspects of the theory of spin relaxation by nematic director fluctuations. A complete review of the theory can be found in Ref. [9] and references therein.

Let us define two Cartesian coordinate systems: D (X,Y,Z) (director/laboratory frame) and d (α,β,γ) (micellar frame) [6], such that the Z and γ axes are oriented [10] along $\hat{\mathbf{n}}_o$ and $\hat{\mathbf{n}}(\mathbf{r})$, respectively.

The NMR spin-lattice relaxation rate is obtained from Bloembergen, Purcel, and Pound theory [11] as

$$T_1^{-1} = K_D[J_1(\nu_L) + J_2(2\nu_L)], \tag{1}$$

where $K_D = \frac{9}{8}(\gamma^2 \mu_0 \hbar / 4\pi r^3)^2$ describes the dipolar interaction and $J_1(\nu_L)$, $J_2(2\nu_L)$ are the spectral densities [12]. In the case of a specific molecular motion where the internuclear distance r is considered fixed, T_1 is obtained from the determination of $J_1(\nu_L)$, $J_2(2\nu_L)$.

Considering $\hat{\mathbf{n}}_o \| Z$ (in the presence of $\mathbf{B} = B_o \hat{\mathbf{z}}$) the fluctuations at any point $\mathbf{r}$ are described by $\delta\mathbf{n}(\mathbf{r},t)$, with orientational components $\delta n_\beta(\mathbf{r},t)$ $(\beta = X,Y)$. $\hat{\mathbf{n}}(\mathbf{r},t)$ can be expressed as

$$\hat{\mathbf{n}}(\mathbf{r},t) = \hat{\mathbf{n}}_o + \delta\mathbf{n}(\mathbf{r},t). \tag{2}$$

The correlation functions associated to this mechanism are written as [13–16]

$$G_{\mathrm{OFD}}(t) = \langle \delta\mathbf{n}(\mathbf{r},0)\, \delta\mathbf{n}(\mathbf{r},t) \rangle, \tag{3}$$

where OFD states for orientational fluctuations director.

The contribution to the spectral density is

$$J_1(\omega_o) = S^2 r^{-6} \mathrm{Re} \int_{-\infty}^{\infty} \langle \delta\mathbf{n}(\mathbf{r},0)\, \delta\mathbf{n}(\mathbf{r},t) \rangle\, dt, \tag{4}$$

where S is the nematic scalar order parameter and $\omega_o = 2\pi\nu_L$.

Writing $\delta\mathbf{n}(\mathbf{r},t)$ in an appropriate diagonal basis set in the reciprocal space, the uncoupled transversal modes $\delta\mathbf{n}_\alpha(\mathbf{q})$ $(\alpha = 1,2)$, which give the instantaneous equilibrium orientation of the director (with an exponential damped relaxation) [16], is written as

$$\delta\mathbf{n}_\alpha(\mathbf{q},t) = \delta\mathbf{n}_\alpha(\mathbf{q},0) \exp\left[-\frac{|t|}{\tau_\alpha(\mathbf{q})} \right], \tag{5}$$

$$\tau_\alpha^{-1}(\mathbf{q}) = \frac{K_\alpha(\mathbf{q})}{\eta_\alpha(\mathbf{q})} q^2, \tag{6}$$

where τ_α and K_α are the damping and curvature elastic constants, respectively, and η_α is the viscosity.

Carrying out the time integration of Eq. (4) in the reciprocal space, the resulting contribution to the spin relaxation rate can be analyzed in two limiting cases.

(i) In the case of nematics where the anisotropy of the elastic constants can be neglected (i.e., $K_{11} \approx K_{22} \approx K_{33} \approx K$) [15], it is assumed isotropic OFD elastic perturbations, and the spin-lattice relaxation is $T_1^{-1} \propto \nu_L^{-1/2}$.

(ii) Introducing anisotropic viscoelastic coefficients and using the case where $K_{11} \approx K_{22} \gg K_{33}$ (bidimensional OFD), Vilfan *et al.* [15] and then Vold and Vold [17] found $T_1^{-1} \propto \nu_L^{-1}$, being this expression usually employed to study OFD's in smectics [18].

In the general case where the viscoelastic coefficients allow $\mathbf{q}$ to assume values in a general ellipsoidal volume in the

reciprocal space, far away from the cutoff limits, the dispersion relaxation could be written in a generalized form by means of a power law,

$$T_1^{-1} \propto \nu_L^{-\rho} \quad \text{with} \quad 1/2 \leqslant \rho \leqslant 1. \tag{7}$$

The angle specifying the orientation of the director $\hat{\mathbf{n}}(\mathbf{r})$ with respect to the D frame fluctuates with time. These fluctuations can be identified with two dynamical processes [19]: (i) translational diffusion of the micelles in a static director field (corresponding to a micellar diffusion coefficient $D_{mic} \gg K/\eta$), and (ii) translationally immobile spins subject to viscoelastic director fluctuations ($D_{mic} \ll K/\eta$). In the case of lyotropics, $D_{mic} \sim 10^{-6}$ cm^2/s, $\eta \sim 1$ P [20] and $K \sim 10^{-6}$ dyn [21] and $D_{mic} \approx K/\eta$. So, in this case, both processes occur. In order to include both dynamical processes, the translational diffusion constant is included in the damping constant [Eq. (6)] [9],

$$[\tau_\alpha^{-1}(\mathbf{q})_{eff}] = \left[\frac{K_\alpha(\mathbf{q})}{\eta_\alpha(\mathbf{q})} + D_{mic}\right] q^2. \tag{8}$$

With the effective damping constant, the cutoff frequencies are defined as

$$\nu_j = [\tau_\alpha^{-1}(\mathbf{q})_{eff}], \tag{9}$$

with $q_j = 2\pi/\lambda_j$ and j = HC (High Frequency) or LC (Low Frequency).

B. $T_1(\nu_L)$ of micellar protons fitting procedure

As a general rule, experimental $T_1^{-1}(\nu_L)$ profiles of the micellar protons, irrespective to the temperature and water concentration, are described by two relevant relaxation mechanisms $T_{1(IM)}$ and $T_{1(OFD)}$: *Individual molecule or tails reorientational mechanism* (IM) and OFD, respectively. Both separately dominate $T_1^{-1}(\nu_L)$ in two different Larmor frequency ranges [4].

Range I: At low ν_L's i.e., $\nu_L \lesssim 10^5$ Hz—the expressions that will be used to fit experimental $T_1^{-1}(\nu_L)$ data are [22]

$$T_1^{-1}(\nu_L) \approx T_{1(OFD)}^{-1}(\nu_L) = \Delta f_{OFD}(\nu_L, \nu_{LC}, \nu_{HC}) \nu_L^{-\rho}, \tag{10}$$

where

$$f_{OFD}(\nu, \nu_{LC}, \nu_{HC}) = 1 - G_{LC} - G_{HC}, \tag{11}$$

$$G_{LC} = -\frac{1}{\pi}\left[\tan^{-1}\left(\frac{\sqrt{\frac{2\nu_L}{\nu_{LC}}}}{\frac{\nu_L}{\nu_{LC}} - 1}\right) + \tanh^{-1}\left(\frac{\sqrt{\frac{2\nu_L}{\nu_{LC}}}}{\frac{\nu_L}{\nu_{LC}} + 1}\right)\right] + \Theta(\nu_{LC} - \nu_L), \tag{12}$$

$$G_{HC} = \frac{1}{\pi}\left[\tan^{-1}\left(\frac{\sqrt{\frac{2\nu_L}{\nu_{HC}}}}{\frac{\nu_L}{\nu_{HC}} - 1}\right) + \tanh^{-1}\left(\frac{\sqrt{\frac{2\nu_L}{\nu_{HC}}}}{\frac{\nu_L}{\nu_{HC}} + 1}\right)\right] + \Theta(\nu_L - \nu_{HC}), \tag{13}$$

and Θ is the Heaviside function. ρ, Δ are the high (HC) and low (LC) cutoff frequencies are the fitting parameters.

Range II: In the high frequencies range ($\nu_L \gtrsim 10^5$ Hz), the data were fitted by two Debye-type functions $L_i(\nu, \tau_i), i = 1,2$ with different weights Φ_1 and Φ_2 and reorientation time constants τ_1 and τ_2,

$$T_1^{-1}(\nu_L) \approx T_{1(IM)}^{-1}(\nu_L) = \Phi_1 L_1(\nu_L, \tau_1) + \Phi_2 L_2(\nu_L, \tau_2). \tag{14}$$

The two Debye-type functions are written as

$$L_i(\nu_L, \tau_i) = \tau_i \sum_{p=1}^{2} \frac{p^2}{1 + \left(\frac{1}{3} p \pi \nu_L \tau_i\right)^2}, \qquad i = 1,2. \tag{15}$$

C. Deuterium NMR quadrupolar splitting

If the water molecules reorientational motion is slow compared to the residual quadrupolar interaction $\mathcal{H}_s(t)$, the first order spectrum for spin $I = 1$ (^{2}H case) consists of two equally spaced lines (centered at ν_o) with a spectral separation, referred to as *the quadrupole splitting*, given by

$$\Delta\nu(\theta) = \frac{3}{4}\kappa |(3\cos^2\theta - 1)A|, \tag{16}$$

where $\kappa = e^2 Qq/\hbar = 246$ kHz [23] is the quadrupolar coupling constant, q is the maximum value of the electric field gradient at the deuterium sites, Q is the deuterium electric quadrupole moment, θ is the angle between the magnetic field **B** and the electric field gradient axis, and A is the residual quadrupolar anisotropy that is related to the order parameter. The singlet spectrum is recovered just when the isotropic water reorientations are enough to average $\mathcal{H}_s(t)$.

IV. RESULTS AND DISCUSSION

A. ^{2}H-NMR line shapes

Figures 1(a)–1(f) show the quadrupolar splitting of the ^{2}H in the sample labeled TD2. The labels (a–f) correspond to different sample temperatures. We show only the results obtained with TD2 sample since it has wider ranges for the exhibited phases as a function of the temperature. Similar results were obtained with samples TD1 and TD3. The sequence of temperatures and the correspondence between phases and splitting are (a) ISO_1/45 °C—singlet; (b) coexisting ISO_1 and N_C/40 °C—doublet superimposed with an isotropic singlet; (c) N_C/30 °C—simple doublet; (d) N_B/18 °C—simple doublet; (e) N_D/15 °C—doublet superim-

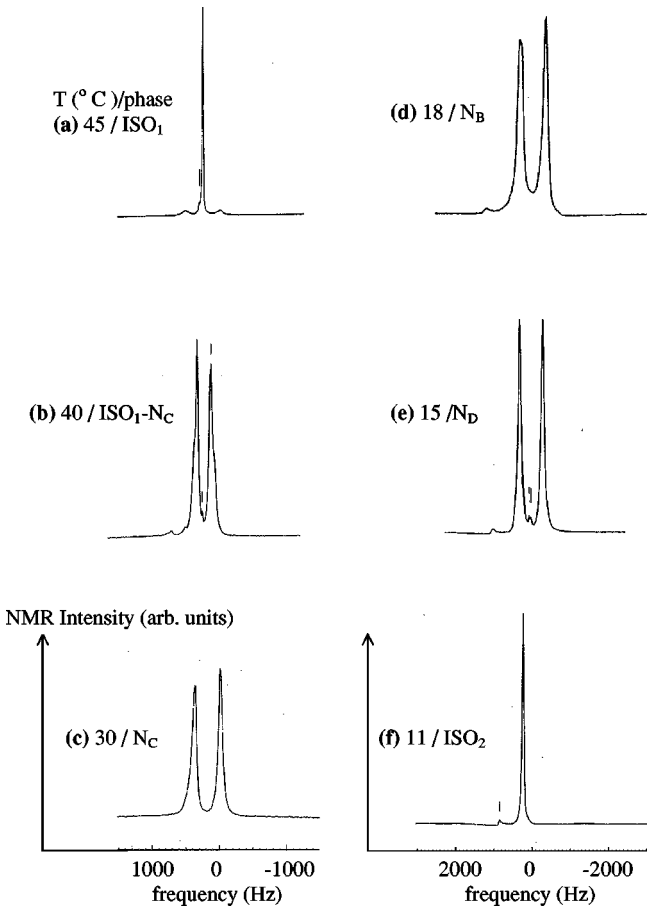

FIG. 1. ^{2}H NMR spectra of D_2O in TD2 sample. (a) ISO_1, T $=45\,°C$; (b) coexistence of ISO_1 and N_C, T$=40\,°C$; (c) N_C phase, T$=30\,°C$; (d) N_B phase, $T=18\,°C$; (e) N_D phase, T$=15\,°C$ and (f) ISO_2 phase, T$=11\,°C$.

posed with an isotropic singlet; (f) ISO_2/11°C—singlet. A summary of these results is shown in Table II.

The presence of doublets or quadrupolar splitted deuterium NMR spectra—indicates that the water reorientations are not enough to completely average the ^{2}H quadrupolar Hamiltonian. On the contrary, the presence of singlet in the ISO phases indicates that, in the NMR time scale, isotropic reorientations of water molecules average the deuterons quadrupolar interactions. In other words, the electric field gradient at the deuterium nuclei sites is averaged to zero in the ISO phases, while it remains nonzero in the nematic ones. The presence of the doublets in the nematic mesophases is compatible with the assumption that the water molecules experience only one axial rotation. Moreover, the simple doublet means that both ^{2}H nuclei of a water molecule are chemically equivalent, sensing each one the same electric field gradient.

TABLE III. Factor $f=K_Q/K_D$ defined in the text.

TD1	TD2	TD3
$f=7.5$ at 20 °C	$f=6.5$ at 20 °C	$f=9.0$ at 20 °C
$f=7.5$ at 30 °C	$f=7.0$ at 30 °C	$f=7.0$ at 30 °C
$f=8.0$ at 45 °C	$f=7.0$ at 45 °C	$f=8.0$ at 45 °C

These experimental results will be discussed on the basis of the following microscopic picture. The space between micelles is enough to acommodate only about five water hydration layers. Due to this reduced intermicellar space, the diffusion path for the spin-bearing species, such as water or counterions, can be consider as being two-dimensional (2D), i.e., the translational motion of these molecules can be treated as a bicontinue surface diffusion process. Furthermore, the hydrophilic electric interaction between water molecules and the surface of the micelles constitutes an additional motional constraint on water reorientations.

Let us consider the water dynamics as a two-steps process [7]: a local anisotropic fast reorientation superimposed to a long-range slow motion. This picture is quantified in terms of the probability distribution function $P(\Omega)$ for the Eulerian angles Ω specifying the transformation between two reference frame axis. One of them (hereafter named M) is attached to the water molecule, with the z axis parallel to the C_2 symmetry axis of the molecule. The other one, the micellar surface coordinate system (d), is fixed to the micelle, with the γ axis (referred to as the local director) perpendicular to the local micellar surface. The external static magnetic field defines the Z direction of the laboratory coordinate frame axes (D). In this framework, the motion giving rise to the time dependence in $\Omega_{dD}(t)$ and $\Omega_{dM}(t)$, occurs at different time scales. So, Ω_{dD} remains essentially constant over large enough time for the statistical averaging of Ω_{dM}. In other words, fast and slow motions are assumed to be statistically independent. A possible mechanism for the fast motion was suggested by Woessner [24] as a fast rotation of water

TABLE II. Summary of the results of the quadrupolar water spectra measurements in all phases showing the sample, temperature and splitting with the following notation: (*) singlet; (**) simple doublet; (***) doublet with structure; (****) doublet superimposed with an isotropic singlet.

TD1	TD2	TD3
(a) ISO_1/45 °C (*)	(a) ISO_1/45 °C (*)	(a) ISO_1/45 °C (*)
(b) N_B/30 °C (**)	(b) ISO_1-N_C/40 °C (****)	(b) N(**)
(c) POL/18 °C (**)	(c) N_C/30 °C (**)	(c) N_B/20 °C (***)
(d) ISO_2/7 °C (*)	(d) N_B/18 °C (**)	
	(e) N_D/15 °C (****)	
	(f) ISO_2/11 °C (*)	

around the C_2 axis with correlation time τ_{rot}. This thermally activated mechanism was already observed in water relaxation in lipids by Cornell *et al.* [23]. The slow motion is conceived as a translational diffusion of water molecules between different environments with correlation time τ_{diff} comparable to the micellar collective (OFD undulation) modes.

In this model, the quadrupolar Hamiltonian can be splitted in two time-dependent parts—slow ($\mathcal{H}_s$) and fast ($\mathcal{H}_f$) dependence—each one accounting for the two steps of motional averaging of the quadrupolar interaction.

1. ^2H spectra of water in nematic phases

These phases are characterized by a long-range correlation order among micelles. As proposed in Ref. [6], the symmetries of the three different nematic phases are obtained through different micellar orientational fluctuations. X-ray results [1] showed that micelles are organized in a pseudolamellar structure with a positional correlation between micelles along the perpendicular direction of the amphiphilic bilayer. In this picture, water molecules, during their diffusion through the sample, maintain (on average) their C_2 axis always perpendicular to the micellar surface. The simple doublets depicted in Figs. 1(c)–1(e) can be interpreted by assuming that their C_2 axis simply diffuse through a roughly plane micellar surface. The motion that spatially modulates $\Omega_{dD}(t)$ should be slow as compared with the residual quadrupolar interaction $\mathcal{H}_s(t)$. In summary, the water dynamics in the nematic phases seems to be composed by two independent motions: (i) fast free rotations along the C_2 axis and (ii) the slow reorientations of its C_2 axis, possible due to the water diffusive process through the micellar pseudolamellar ordering [25].

2. ^2H spectra of water in isotropic phases

Following the above described model the singlet observed in Figs. 1(a) and 1(f), indicate that the isotropic reorientations of the C_2 axis are fast enough to average the quadrupole interactions. In the framework of the pseudolamellar local organization of micelles, even in the isotropic phase in the vicinity of the nematic domain, the water molecules mean-free path is significantly larger than the typical coherence length [20] of the micellar correlation volume.

B. ^{2}H-longitudinal relaxation dispersion $T_1(\nu_L)$

Both ^{2}H and ^{1}H, $T_1(\nu_L)$ relaxation dispersions are presented in Figs. 2, 3, and 4, corresponding to samples TD1, TD2, and TD3, respectively. In each figure, the open circles correspond to ^{2}H relaxation of the intermicellar deuterated water molecules and the filled circles to the ^{1}H relaxation of KL and DeOH molecules of the micelles. At a given sample and temperature both measurements have been made in order to compare directly the correspondence between water (^{2}H) and micellar (^{1}H) dynamics. Solid lines are the fit of experimental $T_1(\nu_L)$ of the micellar protons to Eqs. (10) to (15) (see Table I and Table II in Ref. [4] for the fitting parameters). The measured heavy water deuterium $T_1(\nu_L)$ is fitted

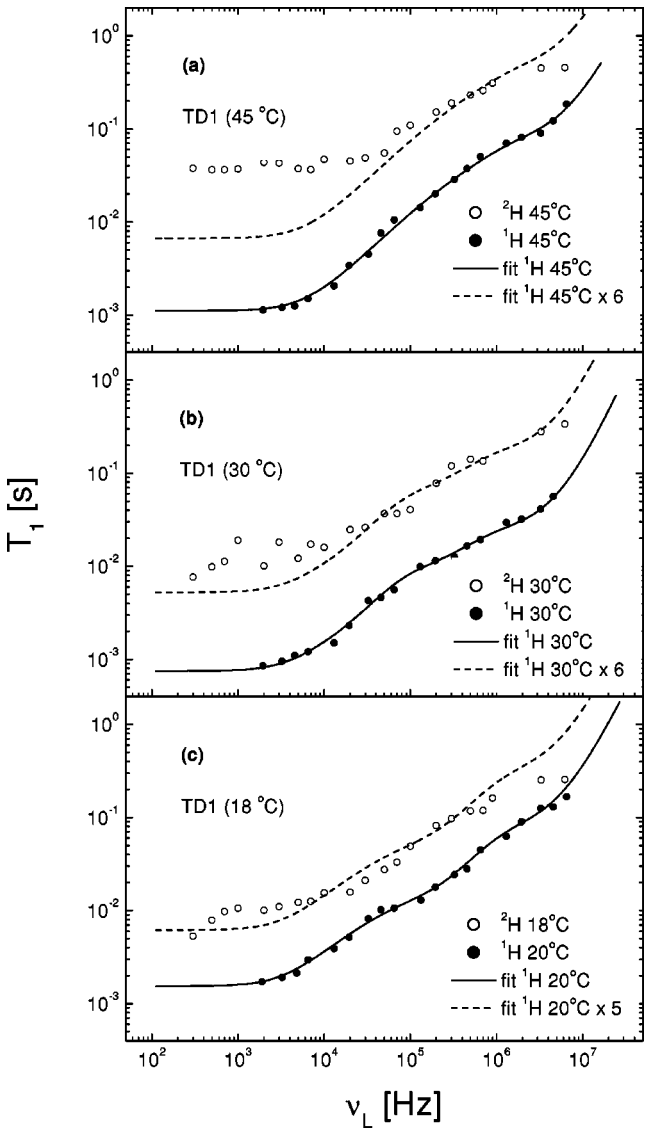

FIG. 2. $T_1(\nu_L)$ profiles of ^{2}H and ^{1}H relaxation dispersion of TD1 sample. The solid lines represent the fitting with Eqs. (10) to (15). Dashed lines have been obtained multiplying the solid line fitting by a factor $f=K_Q/K_D$, see Eq. (18). (a) $T=45$ °C (ISO_1 phase); (b) $T=30$ °C (N_B phase) and (c) 18 °C (POL phase).

by a function (dash line) that is simply the product of the micellar protons $T_1(\nu_L)$ fitting function (solid line) by a constant value *f*, in between 5 and 9. Except for Fig. 2(a), where the dash line does not fit at all the experimental data, the proportionality in between the spin-lattice dispersions curves of micellar protons and water deuterium is clearly verified in practically the whole and broad Larmor frequency range, from 10^2 to 10^7 Hz. See Table III.

The $T_1(\nu_L)$ relaxation dispersion of a quadrupolar and a dipolar system are, respectively [12],

$$T_{1Z}^{-1}=K_D[J_1(\nu_L)+J_2(2\nu_L)], \tag{17}$$

$$T_{1Q}^{-1}=K_Q[J_1(\nu_L)+J_2(2\nu_L)],$$

where $J_1(\nu_L)$, $J_2(2\nu_L)$ are the spectral densities of the spin

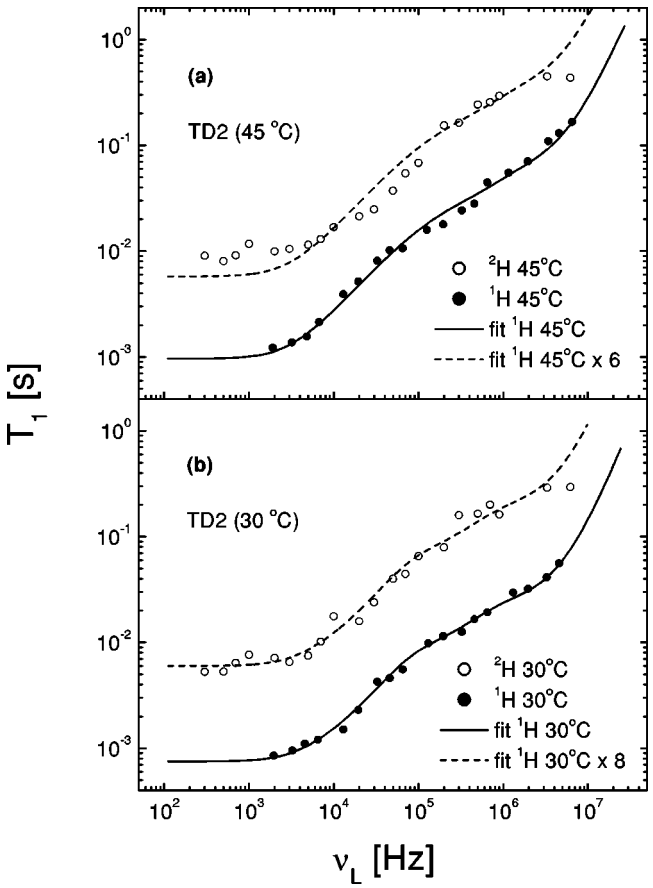

FIG. 3. $T_1(\nu_L)$ profiles of ^{2}H and ^{1}H relaxation dispersion of TD2 sample. The solid lines represent the fitting with Eqs. (10) to (15). Dashed lines have been obtained multiplying the solid line fitting by a factor $f=K_Q/K_D$, see Eq. (18). (a) $T=45\,^\circ$C (ISO_1 phase) and (b) $T=30\,^\circ$C (N_C phase).

pair reorientations. The dipolar and quadrupolar scale coefficients are, respectively, $K_D=\frac{9}{8}(\mu_o/4\pi)^2\gamma_p^4\hbar^2/r^6$ and $K_Q=\frac{3}{80}(e^2qQ/\hbar)^2(1+\eta^2/3)$. μ_o is the vacuum permittivity, γ_p the proton magnetogiric ratio, r the average interprotons distance (in our case, the protons in the paraffinic chains of KL and DeOH molecules), q the maximum electric field gradient at the water deuterium sites, Q the deuterium quadrupole moment, and η the water asymmetry parameter of the oxygen-deuterium chemical bond.

Considering Eq. (18) and the proportionality between the measured $T_1(\nu_L)$ of ^{2}H and ^{1}H, we have

$$\frac{T_{1Z}^{-1}}{T_{1Q}^{-1}}=\frac{K_D}{K_Q}. \tag{18}$$

This means that the *low frequency spectral density* of the micellar protons is equivalent to that of water deuterons. Plugging numbers on Eq. (18) and assuming $r=2.6\times10^{-10}$ m (see Refs. [4,26]) and $(1+\eta^2/3)=0.0014$ [7,27,28], one obtains $T_1^{2H}/T_1^{1H}\approx8$, which gives the order of magnitude of the factor f defined above.

Let us analyze now Fig. 2(a), which was obtained in the ISO phase far (13 °C) from the transition to the nematic

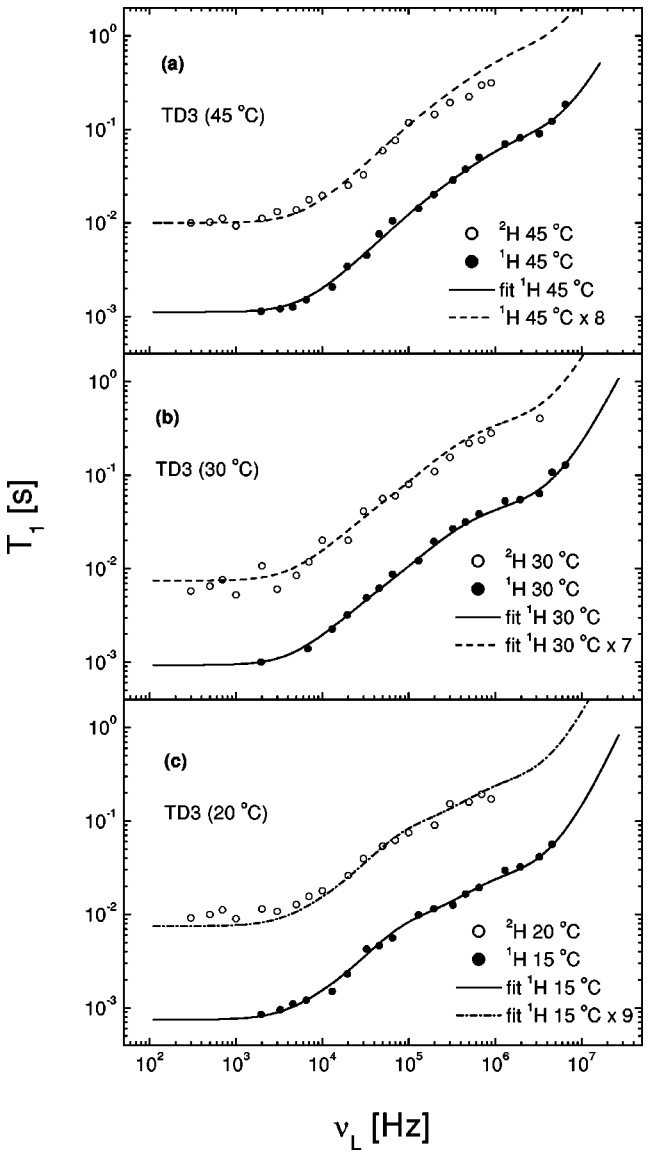

FIG. 4. $T_1(\nu_L)$ profiles of ^{2}H and ^{1}H relaxation dispersion of TD3 sample. The solid lines represent the fitting with Eqs. (10) to (15). Dashed lines have been obtained multiplying the solid line fitting by a factor $f=K_Q/K_D$, see Eq. 18). (a) $T=45\,^\circ$C (ISO_1 phase), (b) $T=30\,^\circ$C (N_C phase), and (c) $T=20\,^\circ$C (N_B phase).

phase. The T_{1Z} profile of ^{1}H is identical to the other obtained in the nematic phases. This indicates that, even at that temperature, the *local* micellar nematic ordering remains. On the contrary, the ^{2}H profile deviates from the proportionality behavior and become almost constant at low Larmor frequencies. The constant $T_1(\nu_L)$ profile means that the water molecules isotropically reorient [29].

V. CONCLUSIONS AND FINAL REMARKS

Two principal features are observed from the experiments: (i) in both, nematic and isotropic phases, the protons and deuterons T_1 dispersion curves are parallel in the log-log plot, except in the water deuterons at the isotropic phase at temperatures far from the nematic to isotropic phase transi-

tion; (ii) in the nematic phases the deuterons NMR spectra is composed by a doublet, meanwhile in the isotropic phases singlet spectra is observed. These features indicate that: (i) the slow reorientational motions of the water deuteron-deuteron axis and the interproton axis of the micellar aliphatic chains are strongly correlated; (ii) water is not characterized by isotropic rotations in the intermicellar volume.

Due to the fact that there are about five or six water layers between micelles, they are considered, from the NMR point of view, as constituting a unique class. All water molecules strongly interact with the polar heads of the amphiphilic molecules forming micelles and our results support the proposition to discard any bulk mediated effect in the relaxation processes [29]. Water molecules, while diffusing along the interface, rapidly rotate around their C_2 axis with a correlation time τ_{rot} and, at the same time, reorient their C_2 with a correlation time τ_{diff}.

In nematic phases micelles are organized in a pseudolamellar structure with long-range orientational correlation. In this way, water molecules sense an approximately flattened regular charged surface during their translational diffusion, keeping their C_2 axis essentially perpendicular to the micelle surface. Within this framework, the maximum electric field gradient direction at the deuteron sites remains mainly perpendicular to the interface. Consequently the NMR spectra present a quadrupolar splitting.

In isotropic phases the situation is quite different since micelles present a short-range positional nematic order, with domains of the order of the correlation length, with the local nematic director randomly oriented. In the time scale of the NMR the water molecules diffuse through many domains with directors randomly oriented, therefore, their C_2 axes experience isotropic rotations. Consequently, the deuterons quadrupolar splitting collapses in a single line.

Line shape results are consistent with the model of biaxial platelet shaped micelles [6]. If micelles had ellipsoidal shaped, water diffusion should average the quadrupolar moment to zero even in nematic phases. In that case the angle between the maximum electric field gradient direction and the external magnetic field (**B**) should have all values between 0 and 2π.

ACKNOWLEDGMENTS

The authors thank the Argentine National Research Councils CONICET, the National Agency for Science and Technology ANPCyT, and the Córdoba Province Science Agency FAPESP, PRONEX, and CNPq from Brazil partially financed this project.

[1] A.M. Figueiredo Neto, in *Phase Transitions and Complex Fluids*, edited by P. Tolédano and A. M. Figueiredo Neto (World Scientific, Singapore, 1998), p. 151.
[2] J.G. Watterson, Mol. Cell. Biochem. **79**, 101 (1988).
[3] C.L. Khetrapal, A.C. Kunwar, A.S. Tracey, and P. Diehl, NMR Basic Principles Progress **9**, 1 (1975).
[4] C.R. Rodríguez, F. Vaca Chávez, D.J. Pusiol, A.M. Figueiredo Neto, and R.-O. Seitter, J. Chem. Phys. **113**, 10 809 (2000).
[5] A.M. Figueiredo Neto, L. Liébert, and Y. Galerne, J. Chem. Phys. **89**, 3737 (1985).
[6] Y. Galerne, A.M. Figueiredo Neto, and L. Lièbert, J. Chem. Phys. **87**, 1851 (1987).
[7] B. Halle and H. Wennerström, J. Chem. Phys. **75**, 1928 (1981).
[8] R.-O. Seitter and R. Kimmich, *in Encyclopedia of Spectroscopy and Spectrometry* (Academic, London, 1998).
[9] R.Y. Dong, *Nuclear Magnetic Resonance of Liquid Crystals* (Springer, Heidelberg, 1994).
[10] F. Vaca Chávez, F. Bonetto, and D.J. Pusiol, Chem. Phys. Lett. **330**, 368 (2000).
[11] N. Bloembergen, E.M. Purcell, and R.V. Pound, Phys. Rev. **73**, 679 (1948).
[12] A. Abragam, *The Principles of Nuclear Magnetism* (Clarendon, Oxford, 1961).
[13] R. Blinc, M. Luzar, M. Vilfan, and M. Burgar, J. Phys. Chem. **63**, 3445 (1975).
[14] R. Blinc, NMR Basic Principles Progress **13**, 97 (1976).
[15] M. Vilfan, M. Kogoj, and R. Blinc, J. Phys. Chem. **86**, 1055 (1987).
[16] P.G. de Gennes and J. Prost, *The Physics of the Liquid Crystals*, 2nd ed. (Clarendon, Oxford, 1993).
[17] R.R. Vold and R.L. Vold, J. Chem. Phys. **88**, 4655 (1988).
[18] F. Noack, *Encyclopedia of Spectroscopy and Spectrometry* (Ref. [8]).
[19] B. Halle, P.-O. Quist, and I. Furó, Phys. Rev. A **45**, 3763 (1992).
[20] P.R. Fernandes and A.M. Figueiredo Neto, Phys. Rev. E **56**, 6185 (1997).
[21] T. Kroin, A.J. Palangana, and A.M. Figueiredo Neto, Phys. Rev. A **39**, 5373 (1989).
[22] J. Struppe and F. Noack, Liq. Cryst. **20**, 595 (1996).
[23] B.A. Cornell, J.M. Pope, and G.J.F. Troup, Chem. Phys. Lipids **13**, 183 (1974).
[24] D.E. Woessner, J. Chem. Phys. **36**, 1 (1962).
[25] A.M. Figueiredo Neto, Y. Galerne, A.M. Levelut, and L. Liébert, J. Phys. (France) Lett. **46**, L-499 (1985).
[26] W. Kühner, E. Rommel, and F. Noack, Z. Naturforsch. **42a**, 127 (1987).
[27] D.T. Edmonds and A. Zussman, Phys. Lett. **41A**, 167 (1972).
[28] J.C. Hindman, A.J. Zielen, A. Svirmickas, and M. Wood, J. Chem. Phys. **54**, 621 (1971).
[29] R. Kimmich, *NMR Tomography, Diffusometry, Relaxometry* (Springer-Verlag, Berlin, 1997).